Laser-induced desorption of NO from NiO(100): *Ab initio* calculations of potential surfaces for intermediate excited states

Cite as: J. Chem. Phys. **104**, 10030 (1996); https://doi.org/10.1063/1.471747
Submitted: 03 August 1995 • Accepted: 22 March 1996 • Published Online: 31 August 1998

T. Klüner, H.-J. Freund, J. Freitag, et al.

Laser-induced desorption of NO from NiO(100): *Ab initio* calculations of potential surfaces for intermediate excited states

T. Klüner and H.-J. Freund
Lehrstuhl für Physikalische Chemie I, Ruhr-Universität Bochum, Universitätsstr. 150, 44780 Bochum, Germany

J. Freitag and V. Staemmler
Lehrstuhl für Theoretische Chemie, Ruhr-Universität Bochum, Universitätsstr. 150, 44780 Bochum, Germany

(Received 3 August 1995; accepted 22 March 1996)

In order to interpret the experimental results of the state resolved UV-laser-induced desorption of NO from NiO(100) (rotational and vibrational populations, velocity distributions of the desorbing NO molecules, etc.), we have performed *ab initio* complete active space self-consistent field (CASSCF) and configuration interaction (CI) calculations for the interaction potential between NO and the NiO(100) surface in the electronic ground state and for those excited states which are involved in the desorption process. The NiO(100)–NO distance and the tilt angle between the NO axis and the surface normal have been varied. A cluster model containing a NiO_5^{8-}-cluster embedded in a Madelung potential has been used for representing the NiO(100) surface. The excited states which are important for the desorption process, are charge transfer states of the substrate–adsorbate system, in which one electron is transferred from the surface into the NO-2π-orbital. The potential curves of these excited charge transfer states show deep minima (4 eV–5 eV) at surface/NO distances which are smaller than that in the ground state. The angular dependence of these potentials behaves similar as in the ground state. A semiempirical correction to the calculated excitation energies has been added which makes use of the bulk polarization of NiO. With this correction the charge transfer states are considerably stabilized. The lowest excitation energy amounts to about 4 eV which is in reasonable agreement with the onset of the laser desorption observed experimentally at about 3.5 eV. The density of the NO^--like states is rather high, so that probably several excited states are involved in the desorption process. The potential energy curves for all of these states are quite similar, but the transitions from the ground state into different excited charge transfer states show strongly differing oscillator strengths, which are also strongly dependent on the surface/NO distance. This fact is important for the dynamics of the deexcitation process in the sense of a selection criterion for the states involved. The magnitude of the oscillator strengths is large in comparison with the excitation of NO in the gas phase, which might be an indication for the possibility of optical excitation processes. One dimensional wave packet calculations on two potential energy curves using fixed lifetimes for the excited state in each calculation have been performed and enable us to estimate the mean lifetime of the excited state to be 15 fs$\leqslant\tau\leqslant$25 fs. This implies that the dynamics of the system is dominated by the attractive part of the excited state potential. [S0021-9606(96)02024-7]

I. INTRODUCTION

The laser-induced desorption of small molecules from well characterized surfaces has been a matter of experimental investigations[1–7] and theoretical work for many years but the details of the mechanism are hardly understood, so that often only a rather qualitative picture is used to describe the fundamental processes.

A full theoretical description of such processes requires sufficiently accurate potential energy surfaces for the electronic states involved as well as efficient algorithms for treating the dynamics of the nuclear motion.

As far as the potential surfaces are concerned many investigations have been performed for metal–adsorbate systems such as CO on Ni(100)[8–10] or CO/Pd(100).[11] Mostly rather small cluster models and conventional quantum chemical ab initio methods up to the configuration interaction (CI)- or multiconfiguration self-consistent field (MCSCF) level have been used. However, cluster size effects result in serious problems with respect to the convergence of the calculated properties. A review of the theoretical description of adsorption phenomena in general has recently been published by Sauer *et al.*[12] As has been pointed out by Jennison *et al.*,[13] some progress can be expected for ground states by the use of gradient corrected LDA functionals[14,15] and massively-parallel computer codes.[16] First calculations using these techniques have been presented for NO and NH_3 on Pd (100).[17,18]

Up to now, all *ab initio* calculations for the desorption of small molecules from metal surfaces concentrated on the description of ground state properties, whereas excited states had to be treated semiempirically[17] or totally empirically as in the classical MGR picture.[19,20]

 0021-9606/96/104(24)/10030/11/$10.00

Compared to metals, ionic systems such as NiO(100), exhibit some principal advantages. The strong ionicity allows a local description of the electronic structure at least of the transition metal ion and justifies the use of a rather small cluster compared to calculations on metal surfaces. Thus it is possible to calculate ground state potential surfaces for the adsorption of small molecules such as CO or NO by means of high quality *ab initio* techniques[21,22] including electron correlation effects. In this paper we present the first *ab initio* cluster calculation at the MCSCF/CI level for both *ground and excited states* involved in a desorption induced by electronic transitions (DIET) process. The knowledge of the potential energy surfaces of the excited states is crucial for a deeper insight into the principal mechanism of the desorption process, which should be regarded as one of the most elementary steps in surface photochemistry.

Our present calculations have been stimulated by experiments on the fully state resolved laser-induced desorption of small molecules from different well characterized oxide surfaces, which have been performed in our group during the recent years.[6,23–27] For the system NO on NiO(100) the main experimental results can be summarized as follows:

(a) NO is adsorbed on top of a regular nickel adsorption site.[22,26,28–31]
(b) The binding energy is determined by thermal desorption spectroscopy (TDS) to be 0.52 eV.[26]
(c) The tilt angle between the molecular axis and the surface normal turns out to be 45°.[26]
(d) Desorption experiments were performed with laser energies between 3.5 eV and 6.4 eV; the desorbing NO molecules were analyzed by rotationally and vibrationally state resolved detection. A threshold at about 3.5 eV has been obtained below which the desorption cross section turns out to be very small.[6,25,32,33]
(e) We observed velocity flux distributions of the desorbing NO molecules showing two maxima which can be assigned to two nonthermal desorption channels.[24]
(f) A coupling between rotational and translational degrees of freedom was found in the fast desorption channel.[24]
(g) The vibrational temperature is obtained to be about 2000 K, while rotational temperatures are characteristically much smaller (between 250 K and 450 K).[24]
(h) NO^- is postulated as a probable intermediate during desorption.[24]

While detailed theoretical investigations of the ground state of the NO/NiO(100) system have been presented in an earlier work [22,28,29] we focus in this paper on the excited states involved in the desorption process and we present the results of some calculations for potential energy curves and oscillator strengths. We also have performed preliminary wave packet calculations for the nuclear motion in order to obtain some information about the mean lifetime of the excited states and compared them to the results of classical trajectory calculations.[23]

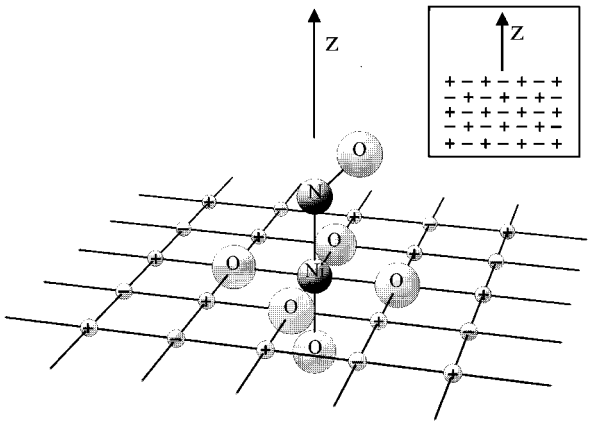

FIG. 1. The NiO_5^{8-}-cluster embedded in a semi-infinite potential of point charges (only the uppermost layer of them is shown). The tilt angle of the NO molecule adsorbed on the cluster is 45° with respect to the surface normal (Ref. 26).

II. METHODS OF CALCULATION

A. Cluster model

The crystal structure of NiO is the same as that of NaCl, which consists of a fcc lattice structure for the Ni^{2+} and O^{2-} ions. The NiO distance is about 2.08 Å[34,35] and each nickel ion is surrounded by six oxygen ions with octahedral symmetry. The NO molecule is adsorbed at the NiO(100) surface in the on-top position on the Ni^{2+} ion with the N atom pointing towards the metal ion. Experimental results (ARUPS) using a thin film of NiO(100) on Ni(100) and a NiO(100) surface of a single crystal cleaved *in vacuo* have shown that there is little dispersion within the Ni $3d$ bands.[26] For this reason one can assume that there exists no direct Ni–Ni interaction. Therefore we have chosen a small cluster as a model system for the NiO(100) surface which contains only one Ni^{2+} ion and five adjacent O^{2-} ions.[21,26] The NiO_5^{8-} cluster is embedded in a semi-infinite Madelung potential which simulates the influence of the bulk ions on the cluster, especially the long-range Coulomb interaction between the ionic lattice and the cluster adsorbate system. The Madelung potential is built up by point charges ± 2; we assume a totally ionic structure and use a modification of the Evjen-summation method.[36] The whole cluster model including an adsorbed NO molecule is shown in Fig. 1.

This cluster model possesses an artificial dipole moment of the order of 1 a.u., caused mainly by the point charges of $+2$ next to the O^{2-} ions which polarize the electron density of the cluster into the direction of the adjacent point charges. In earlier calculations for neutral adsorbate systems like CO, NO, H, and CH_3[21,22,28,37,38] the influence of this artificial dipole moment could savely be ignored, but the interaction between a dipole moment of 1 a.u. and the negative charge of an approaching NO^- ion, which has been proposed as an intermediate, is too large to be neglected. One possible way to eliminate this dipole moment is a modification of the Madelung potential which has been achieved in the following way.[38] All point charges in the first layer are changed to

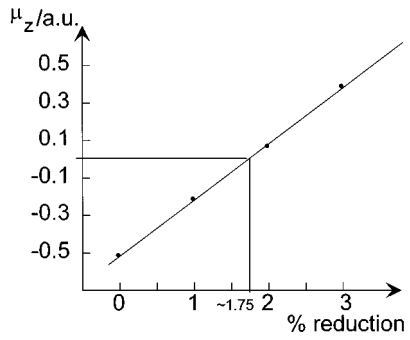

FIG. 2. The dipole moment of the $[Mg_5NiO_5]^{2+}$ cluster in the Madelung field as a function of the reduction of the distance between the first and the second layer.

± 2.4 and in the second layer to ± 2.3, while the rest of the Madelung potential is unchanged. This modification of the Madelung potential produces a change of the electron density towards the positive charges in the first layer and results in a decrease of the dipole moment. There exists no strict definition of the ionicity of an ionic crystal, but charges of ± 2.4 and ± 2.3 for the NiO(100) surface seem to be unphysical, although similar results have been obtained for ZnO by Boussard *et al.*[39] If one considers the Madelung potential as an electrostatic field parametrized for stabilizing the highly negatively charged NiO_5^{8-} cluster and and not as a simulation of true Ni^{2+} and O^{2-} ions of the remaining crystal this model seems to be justifiable.

A different way to reduce the dipole moment is to replace those five positive point charges which are located directly beneath the O^{2-} ions by Ni^{2+} ions or Ni^{2+} pseudopotentials. This prevents a flow of electrons from O^{2-} to the positive charges because of the Pauli repulsion of the Ni^{2+} core. In the present calculations we have used Mg^{2+} instead of Ni^{2+} because it has closed shell structure; on the other hand, the similarities between MgO and NiO (crystal structure, lattice constant, ionicity) justify this approach. Figure 2 shows that the substitution of five point charges by Mg^{2+} ions causes an overcompensation of the artificial dipole moment, however, a relaxation of the distance between first and second layer by about 1.75% leads to a complete disappearance of this artifact. It should be mentioned that all-electron calculations and the use of pseudopotentials for Mg^{2+} yield virtually identical results.

B. Quantum chemical methods

All our *ab initio* calculations have been performed with the Bochum open-shell program package using restricted open shell Hartree–Fock (ROHF),[40] complete active space self-consistent field (CASSCF), and configuration interaction (CI) programs.[41,42] For calculations on the ground state also the coupled electron pair approximation (CEPA),[43] averaged coupled pair functional (ACPF),[44] and multiconfiguration coupled electron pair approximation (MC-CEPA)[45] have been used.

The basis set used consists of the $13s6p4d$ basis of Roos *et al.*[46] for Ni, $7s3p$ of Huzinaga[47] for the O^{2-} cluster ions contracted to DZ quality and the $9s5p$ basis of Huzinaga[47] for the nitrogen and oxygen atoms of the NO molecule and for Mg^{2+}, contracted to TZ quality. The basis of the oxygen ions in the cluster has been extended by adding one semidiffuse s- and p-set with an exponent of 0.1 in order to describe the greater spatial extent of the O^{2-} ions compared to neutral oxygen atoms. For a similar reason, i.e. for a better description of an NO^- ion, the nitrogen and oxygen basis for NO have been extended by one diffuse p-set with the exponents 0.05 and 0.06, respectively.

CI calculations generally require one common set of orbitals from which the reference determinant and all necessary excited configurations can be built up. We have generated such orbitals in two ways. (a) The SCF (=high multiplicity) ground state of the system NiO_5^{8-}–NO^- was calculated at a nickel–nitrogen distance of $R(\mathrm{Ni–N})=5000\ a_0$. This large distance ensures that the orbitals are totally separated into cluster orbitals and NO^--orbitals. This fixed set of orbitals (''frozen SCF orbitals'') was then used in the CI calculations at all shorter distances. (b) CASSCF calculations were performed for the lowest states of the system NiO_5^{8-}–NO at all distances for which CI calculations are to be performed later on. In this method it was necessary to use an average energy expression that includes all components which are needed for correctly describing the $^2\Pi$ ground state of NO interacting with the $^3B_1$ ground state of the cluster.[26,38]

The use of the frozen SCF orbitals of the system NiO_5^{8-}–NO^- in the CI calculations [method (a)] leads to a comparably good description of excited charge transfer states of the form NiO_5^{7-}–NO^-, but to a rather poor description of the ground state of NiO_5^{8-}–NO. Actually, we found nearly no bonding at all with these orbitals, though the experimental binding energy between NO and the NiO(100) surface amounts to 0.52 eV.[26] However, the problem of calculating the NO/NiO(100) binding energy correctly has attracted much attention recently[22,28,29] and is far from being solved. It is therefore not surprising that our procedure (a) which is aiming at a good description of the cluster-to-NO charge transfer states is relatively poor for the ground state. On the other hand, the CASSCF calculations for the lowest states of the ''neutral'' system NiO_5^{8-}–NO [method (b)], yield reasonable ground state orbitals, but describe the NO^--like charge transfer states less accurately than the orbitals generated by the procedure (a). This can be seen if one compares the total energies of these states calculated either with the CASSCF or the frozen SCF orbitals.

The potential curves obtained from the CI calculations with CASSCF orbitals are corrected by the counterpoise method of Boys and Bernardi.[48] To do this we have assumed that the basis set superposition error (BSSE) for the CI ground state and for the excited charge transfer states is the same as that of the CASSCF ground state. In the calculations with the frozen SCF orbitals we did not apply the counterpoise correction since there is no interaction between cluster and adsorbate. After the BSSE correction the shapes of the potential curves calculated with either CASSCF orbitals or

TABLE I. Parameters of Morse potentials and propagation characteristics used in the wave packet calculations.

Parameter	Ground state	Excited state
D_e/a.u.	0.018	0.200
α/a.u.	0.900	0.600
r_0/a.u.	4.5	3.5
potential	$V(r)=D_e\{1-\exp(-\alpha(r-r_0)\}^2$	
m/a.u.	55 085	
grid size/a.u.	0–60 (4096 points)	
Propagation time/a.u.	10 000–50 000	

frozen SCF orbitals show no qualitative differences.

The CI calculations have been performed by including all single and double excitations from the 15 oxygen $2p$ and five nickel $3d$ orbitals into the two NO 2π orbitals starting from a reference determinant, where the oxygen $2p$ orbitals are fully occupied with 30 electrons, the five nickel 3d orbitals contain nine electrons, and the NO 2π orbitals are unoccupied (CISD). This choice was suitable to produce all states of interest and keep the CI-expansion length reasonable short, in the order of about 10 000 determinants per symmetry.

In order to investigate the electronic relaxation of the NiO cluster upon removing one electron, either from the oxygen $2p$ or nickel $3d$ orbitals, different sets of cluster orbitals are generated. Since the $3d^7$ ground state of NiO_5^{7-} is no one-determinant state it has been optimized by CASSCF calculations with the five $3d$ orbitals in the active space and an average energy expression for the three lowest quartet states ($^4A_2$ and ^4E in C_{4v}-symmetry). The resulting set of orbitals shows considerable relaxation only if the additional hole is created in the Ni $3d$ shell. The relaxation effects can be estimated by comparing CI calculations which are performed with either SCF ground state orbitals of the nonionized NiO_5^{8-}-cluster or with the CASSCF orbitals of the ionized NiO_5^{7-}-cluster. The relaxation effects are discussed in more detail in Sec. III.

C. Wave packet dynamics

For the simulation of the nuclear dynamics we started some simple, one dimensional wave packet calculations using the programs of Kosloff and Schmidt based on the Chebychev Propagator developed by Kosloff.[49–54] In these calculations we employed one ground state and one excited state Morse potential curve which have been adjusted to the corresponding *ab initio* curves. The parameters of the potentials and the time propagation characteristics are listed in Table I. We started from the vibrational ground state of the lower potential, obtained numerically by propagation of the wave function in imaginary time, and performed a Franck–Condon-type transition to the excited state potential. After the propagation on this potential for a certain fixed time period the whole wave packet was placed onto the ground state curve, and the ''desorbing'' part of the wave packet was analyzed. This has been done for different fixed lifetimes of the excited state in each calculation. The desorbing part of the wave packet is defined as the probability density which has passed a well defined imaginary border at 12 a.u. on the ground state potential. After this point the potential is sufficiently flat, so that the desorbing part of the wave packet can be regarded as a free particle. In all calculations the time of propagation has been sufficiently long (some 10 000 a.u.) so that a unique separation between the adsorbed and desorbed part of the wave packet has occurred.

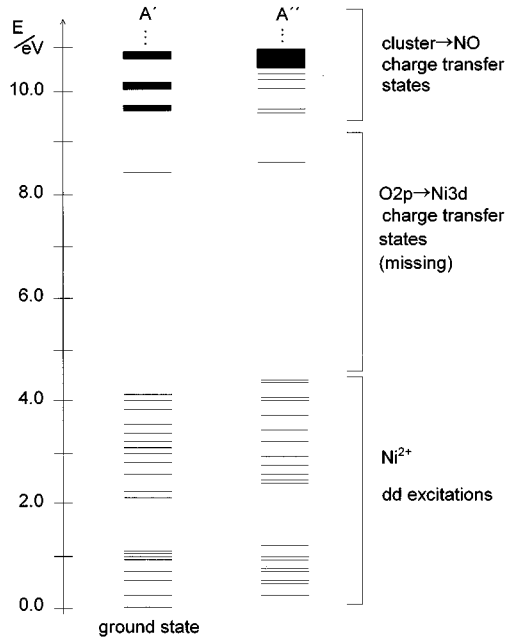

FIG. 3. Overview of the electronic states of the NO/NiO(100) system (CISD with CASSCF-reference) with a nickel–nitrogen distance of R(Ni–N)=5.0 a_0 and a tilt angle of 45°.

III. RESULTS

A. Vertical excitation energies

With the CI calculations as described above it was possible to distinguish between three different types of excited states in the NO/NiO(100) system: local dd-excitations, charge transfer excitations within the cluster, and charge transfer states describing the transfer of one electron from the cluster to the NO molecule.

As shown in Fig. 3 we find a large number of electronic states in the energy range between 0 eV–4 eV, which corresponds to local dd-excitations within the nickel ion. In this energy range, i.e., within the optical band gap, weak signals were measured in the EELS spectrum by Cappus *et al.*[30,31] With the help of *ab initio* calculations performed in our group[30] these signals were associated with the dd-excitations. Above 4 eV a strong increase of intensity is observed in the EELS spectrum, which is interpreted as being due to optically allowed charge transfer transitions of electrons from oxygen to nickel. The states responsible for these transitions cannot be properly described in our calculations, because the choice of a quite small cluster implies (a) a

TABLE II. Vertical excitation energy of the lowest charge transfer ($^4A_2$) state for the linear adsorbed NO molecule using different cluster models and methods of calculation.

Method	Cluster model Madelung field	E/eV at R(Ni–N)=5.0 a_0
CI with frozen SCF orbitals	$[NiO_5]^{8-}$ unmodified Madelung field	6.75
	$[NiO_5]^{8-}$ modified layers[a]	9.52
	$[Mg_5NiO_5]^{2+}$ unmodified Madelung field[a]	6.35
CI with CASSCF orbitals	$[NiO_5]^{8-}$ unmodified Madelung field	9.79

[a]See text Sec. II A.

rather crude description of the delocalized oxygen $2p$-bands and (b) a missing polarization contribution of the bulk NiO crystal which is connected with the generation of charge carriers.[55] As a consequence, the calculated transition energies for these states are several eV too large and are shifted out of the energy range of Fig. 3.

The states involved in the desorption mechanism are charge transfer states in which one electron is transferred from the cluster to the NO-molecule. We observe these charge transfer states above a certain energy threshold which depends on the choice of the orbitals used in the CI calculation. In the following we denote the NO^--like states simply as charge transfer states of the system. Figure 3 shows schematically that the density of these states is quite high and forms a quasicontinuum of which we can obtain only the lower part. The existence of many experimentally accessible states is of crucial importance for the dynamics of the system since several states could be involved in the desorption process. The question how to identify the states which are important for the desorption, will be addressed later in this paper.

Table II contains the excitation energy of the lowest cluster $\rightarrow$ NO charge transfer state as obtained for different orbital spaces in the CI calculations. It can easily be seen that the excitation energy is strongly dependent on the choice of orbitals in the CI. The physical picture behind this result is quite simple. If we use a CASSCF-reference for our CI, those states are well described, which have a similar orbital occupation as the ground state, i.e., which can be characterized as NiO_5^{8-}–NO-like states. Upon charge transfer from the cluster to the NO molecule, large relaxation effects in the electron distribution of both the cluster and the NO molecule are to be expected. Because of the truncated character of our CI calculations, these effects are only partly taken into account and the calculated excitation energy for the lowest excited state is as high as 9.79 eV (at $R=5.0\ a_0$). For a proper description of the charge transfer states, orbital spaces should be used which are constructed for the NiO_5^{7-}–NO^--system. Our CI calculations with the NiO_5^{8-}–NO^- frozen SCF orbitals take the relaxation effects of the NO orbitals during NO^--formation into account, thus a lower excitation energy of 6.75 eV ($R=5.0\ a_0$) is obtained in this case. Since we can only use one orbital set in out present CI calculations, only either the ground state or the NO^--like states are properly described. The relaxation effects within the cluster are still very poorly described, so that the excitation energies are still too high in comparison to the laser energies used in the experiments.[25] However, we were able to estimate these effects by a semiempirical correction of the excitation energies and obtain a reasonable agreement with experiment. This point will be discussed in Sec. III B.

In a similar way as the change in the reference orbitals a modification of the cluster model can also change the vertical excitation energies of the charge transfer states. We find an increase in the lowest excitation energy from 6.75 to 9.52 eV at a Ni–N distance of 5.0 a_0, if we use the modified Madelung potential with higher ionicity, as described above (see Table II). Due to the higher positive charges in the topmost layers the O($2p$) orbitals are stabilized and the charge transfer of one electron from an O($2p$) orbital to NO needs more energy. This is clearly an artifact of the modified Madelung field.

The elimination of the dipole moment by additional magnesium ions produces an opposite effect as far as excitation energies are concerned. The total energies of the ground state and the excited charge transfer states are shifted by about the same amount to higher energies, the excitation energies are only lowered by 0.4 eV from 6.75 to 6.35 eV at $R=5.0\ a_0$. The small amount of 0.4 eV seems to make the correction of the dipole moment unnecessary, but the interaction between dipole moment and the NO^- is strongly distance dependent, therefore the elimination of the dipole moment is important for the correct shape of the potential curves of the excited states.

B. Semiempirical correction of the excitation energies

Quite a difficult question is that of the origin of the electron which is transferred from the surface to the NO molecule, i.e., whether it comes from the O($2p$) or Ni($3d$) orbitals. This problem is closely connected with that of the reliability of Koopmans' theorem. All CI calculations discussed so far in this paper used orbitals which were optimized for the ground state of the ''neutral'' cluster and for either NO^- or NO. However, the charge transfer states are connected with an ionization of the cluster, and there might be rather large relaxation effect since the orbitals of the ionized cluster can be considerably different from those optimized for the ground state of the neutral cluster. Further-

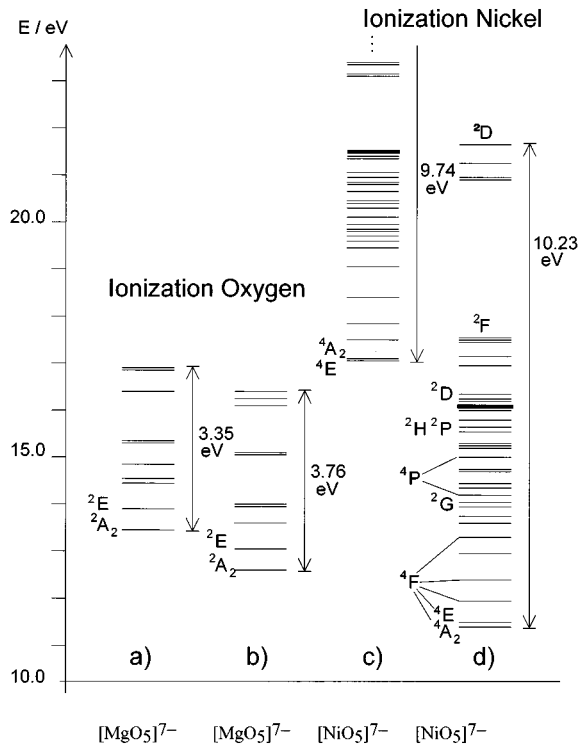

FIG. 4. (a) SCF Koopmans energies of the 15 O $2p$ orbitals. (b) Full-CI in the space of the 15 O $2p$ orbitals optimized in an average of configuration CASSCF calculation for the lowest $^2A_2$, ^2E, and $^2A_1$ states. (c) Full-CI in the space of the 5 Ni $3d$ orbitals optimized in a SCF calculation for the nonionized ground state ($^3B_1$). (d) Full-CI in the space of the 5 Ni $3d$ orbitals optimized in an average of configuration CASSCF calculation for the lowest $^4A_2$ and ^4E states.

more, the relaxation effects might be quite different depending on whether an electron is ionized from a local Ni($3d$)-AO or a delocalized O($2p$) band.

In Fig. 4 we show the ionization energies of NiO obtained with two full CI calculations within the manifold of the $3d^7$ states of Ni^{3+} (this corresponds to a local ionization of Ni^{2+}). In the first calculation [Fig. 4(c)] we used the SCF orbitals of the ''neutral'' nonionized cluster (this corresponds to Koopmans' theorem, but with a valence CI in the ''final'' states). In the second one [Fig. 4(d)] we used CASSCF orbitals optimized for an energy expectation value averaged over the three lowest quartet states of the ionized cluster. Apparently, we find a relaxation energy in the order of 6.5 eV, attributable to the localized hole at Ni.

We have performed similar calculations for the ionization of the oxygen $2p$ orbitals. For technical reasons, these calculations have been performed for a MgO_5 cluster model, which is reasonable because of the great similarities between NiO and MgO. In Fig. 4(a) again the SCF orbitals of the neutral cluster are used (Koopmans' theorem), in Fig. 4(b) orbitals which are optimized for the ionized cluster and which correspond to a delocalized hole within the oxygen $2p$ orbitals. This time we find only a low relaxation energy of about 1 eV. The consequence of the large relaxation of the nickel states upon ionization is that ionization out of the O($2p$) and Ni($3d$) orbitals are very close in energy. This leads to a mixture of $3d^7$- and $3d^8L^{-1}$-configurations for the ground state of the ionized cluster (L^{-1} denoting a hole in the ligand sphere).

In addition to this ''intracluster relaxation''[55] which can be accounted for explicitly by allowing the cluster orbitals to relax upon ionization, there is also an ''extracluster'' polarization, i.e., the polarization of the remainder of the NiO crystal outside the cluster. This is a long-range effect and converges very slowly with the increase of the cluster size, therefore an empirical correction is necessary. Janssen and Nieuwpoort[55] estimated this effect to be in the order of 4–5 eV if an extra point charge is placed at a regular lattice point, e.g., for the ionization out of a strongly localized orbital. Of course, the extracluster polarization is also smaller for the ionization out of a delocalized O($2p$) band.

The low lying electronic states of the ionized NiO_5^{7-} cluster are mixtures of $3d^7$ and $3d^8L^{-1}$-configurations, as Fig. 4 suggests—if relaxation effects are included—and as has been found in previous calculations, e.g., by Janssen and Nieuwpoort[55] or Fujimori and Minami.[56] An analysis of the low lying charge transfer states of the system NiO–NO shows that they contain predominantly configurations that correspond to a charge transfer from O($2p$) to NO.[38] Therefore, the hole created upon this charge transfer is not very strongly localized and a medium value of about 5 eV seems to be a reasonable estimate of the relaxation energy. We have therefore lowered the calculated vertical excitation energies by this amount.

It should be stressed that this semiempirical shift is absolutely necessary since it is not possible to make the cluster large enough and to treat the relaxation completely as intracluster polarization. On the other hand, the form of the potential curves is not changed much and the dynamics is not very sensitive to the exact form of the potential surfaces of the intermediate states.

C. Potential energy curves

In order to characterize the states involved in the desorption process we calculated potential energy curves for the ground state and different charge transfer states on the CI-level. We investigated the dependence of the potential energy on the nickel–nitrogen distance and on the tilting angle with respect to the surface normal.

Figure 5 contains the potential curves of the electronic ground state and two arbitrarily selected NO^--like charge transfer states as functions of the distance between the surface and the adsorbed NO (the semiempirical shift discussed in the the previous section has not been applied). The binding energy of the ground state is strongly underestimated, as has already been pointed out in Sec. II B. However, the exact shape of the ground state potential curve is of minor importance in the present context because the wave packet accumulates kinetic energy mainly by propagation in the excited state potential curves and by conversion of potential energy into kinetic energy after relaxation to the ground state. Thus the final kinetic energy distribution is dominated by the lifetime of the wave packet in the excited state potential and not

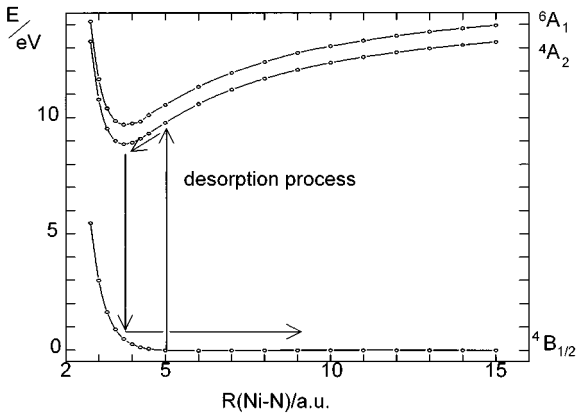

FIG. 5. Potential energy as a function of the cluster NO distance (linear adsorption geometry) for the ground state and two different charge transfer states.

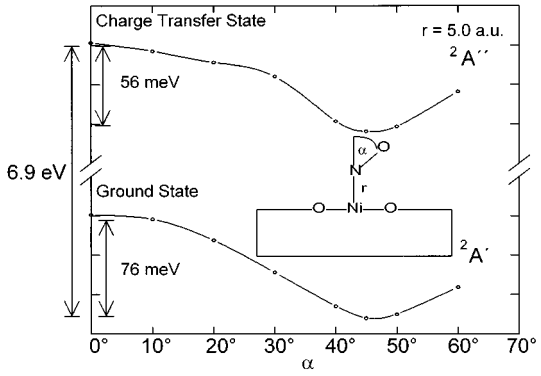

FIG. 6. Angular dependence of energies of the ground state and the lowest excited charge transfer state of the NiO_5^{8-}–NO cluster in the Madelung potential.

by the relatively shallow minimum of the electronic ground state. Therefore, the poor description of the electronic ground state does not change any of our conclusions concerning the desorption process.

As can be seen in Fig. 5, the strong Coulomb interaction between the ionized cluster and the negatively charged NO^- molecule gives rise to pronounced minima with depths of about 5 eV in the potential curves of the charge transfer states. At distances larger than 4.5 a_0 the potential curves of these states are dominated by this strong Coulomb attraction which behaves essentially like $-1/R$, whereas at short distances the potentials are repulsive due to the Pauli repulsion. It is important for the dynamics of the laser-induced desorption process that the equilibrium distances of the NO^--like states are considerably shorter ($R=3.5\ a_0$–$4.0\ a_0$) than that of the ground state ($R=5.0\ a_0$). The situation is comparable to that encountered for an Antoniewicz-type desorption mechanism,[57] which implies that the molecule moves towards the surface immediately after excitation. Another point important for the later discussion is that the potential curves of all excited charge transfer states are very similar.

We have also investigated the influence of the tilt angle between the NO axis and the surface normal on the energies of the different states. Figure 6 contains the angular dependence for the $^2A'$ ground state and the lowest $^2A''$ charge transfer state. In agreement with the experiment the equilibrium tilt angle is found at 45° for the ground state.

So far it is generally assumed that the angular dependence of the potential surfaces is different in the ground and the excited states.[23,58,59] The reason for this assumption was the experimental observation of high translational energies for molecules desorbing with large rotational energy quanta. In contrast to this we find a similar angular dependence of the electronic ground state and the NO^--like excited states. This could be an explanation for the relatively low rotational temperature of the desorbing NO molecules of about 250 K and 450 K as compared to the high vibrational temperature ($T\approx 2000$ K),[25] but that does not account for a straightforward explanation of the coupling of translational and rotational degrees of freedom. Nevertheless, future calculations of the complete potential energy surfaces of the states involved will clarify whether the similarity of the angular potential energies will remain at other distances than the equilibrium Ni/NO-distance, and how the differences in the temperature of rotation and vibration as well as the strong coupling of rotation and translation can be explained.[60]

We want to emphasize that in all our calculations the qualitative aspects remain the same independent of these details and the correct values of the vertical excitation energies. We were able to identify NO^--like charge transfer states as the states which are involved in the desorption process and therefore we agree with the proposal of Gadzuk *et al.*[61] that NO^- is the intermediate during the desorption process.

D. Oscillator strengths

For the simulation of the dynamics of the laser-induced desorption the knowledge of the potential energy surfaces is of primary importance. However, the mechanisms of the excitation and deexcitation processes can only be established if some information on the relaxation probabilities of transitions from the NO^--like intermediate states to the ground state or other excited states of the cluster/adsorbate system describing desorbing neutral NO molecules is available. The mean lifetime of the wave packet in the excited state has to be regarded as a central point of dynamics.

Of course, the question arises whether the primary excitation process as well as the deexcitation after a finite mean lifetime in the excited state is a direct optical process or a substrate excitation followed by a ''hot electron'' being scattered from the surface to NO in a nonadiabatic process and a relaxation via nonadiabatic coupling of the states involved. Because of the short lifetimes of the excited states the direct optical de-excitation was generally ruled out. Lifetimes of optically allowed excited states of gas phase NO are generally in the order of 1–10 ns while estimates for mean lifetimes in the laser induced desorption lead to 15–25 fs (Sec. III E). A rough estimate shows that even with oscillator strengths as large as 0.1 to 1 the radiative lifetimes for spontaneous emission are so large (100 ps–1 ns) that the (radiative) optical de-excitation cannot explain the mechanism for

TABLE III. Oscillator strengths (in units of 10^{-4}) of some selected optically allowed transitions from the ground state into different excited states ($^2A'$ to $^2A'$ transitions). The excitation energies take the artificial dipole moment of the cluster into account and are semiempirically corrected with respect to the intracluster polarization by a uniform shift of 5 eV (see text, Sec. III B).

No.	Excitation energy /eV	$r=5.0$ a.u.
1	3.02	0.14
2	3.08	0.88
3	3.51	0.01
4	3.58	0.01
5	3.59	8.92
6	3.62	12.10
7	4.01	3.39
8	4.03	0.07
9	4.04	0.60
10	4.07	23.92
11	4.14	0.29
12	4.15	0.05
13	4.15	0.04
14	4.32	115.40
15	4.34	4.70
16	4.54	0.02
17	4.65	0.09

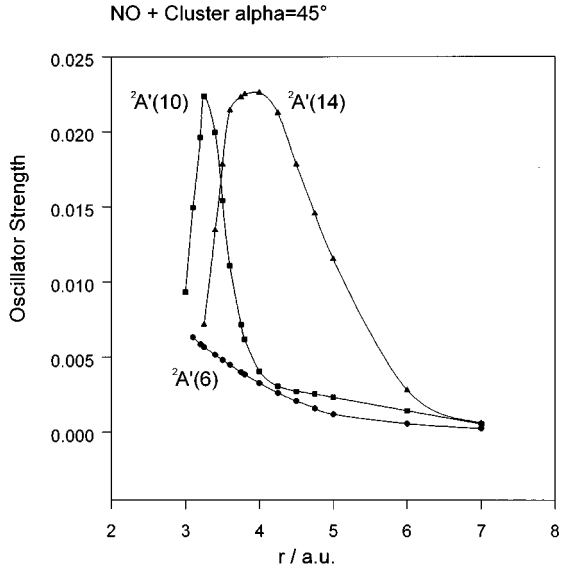

FIG. 7. Distance dependence of oscillator strengths for three optically allowed transitions ($^2A'/^2A'$). The designation of the states is compatible with Table III.

the laser-induced desorption.[60] Therefore future investigations should take the nonradiative de-excitation via the calculation of diabatic coupling coefficients and diabatized potential energy surfaces into account.[60]

Nevertheless, an optical excitation mechanism could in principle take place in competition with the nonadiabatic transitions. We have therefore calculated transition moments and oscillator strengths for optical transitions from the NO/NiO(100) ground state to different charge transfer states. Table III contains the results for the oscillator strengths of the lowest allowed charge transfer states at a Ni–N distance of 5.0 a_0. All excitation energies (necessary for converting the calculated transition moments to oscillator strengths) have been shifted by 5 eV downwards to simulate the effect of the polarization of the whole crystal.

As Table III shows, some of the oscillator strengths are quite large ($\approx 10^{-2}$), much larger than those of the optically allowed transitions of gas phase NO molecules, which are only in the order of 10^{-4}.[62–65] Most of the states possessing large transition moments are characterized by a single electron transfer from a O($2p_z$) or a Ni($3d_{yz}$,$3d_{xz}$) orbital into the partly occupied 2π-orbital of NO, without a change in the spin coupling as compared to the ground state of NO/NiO(100). Figure 7 shows the oscillator strengths of three of the low-lying excited states as functions of the Ni–N distance R. All curves exhibit a nearly exponential decay with increasing R; this is consistent with the nature of these states as single electron charge transfer states and a transition moment of the form $\langle O(2p)|\mu|NO(2\pi)\rangle$ which of course depends on the overlap between the O($2p_z$) and NO(2π) orbitals. For very short distances the behavior of the oscillator strengths becomes irregular because of a strong mixture of different excited states.

The transition moments are quite large at the equilibrium Ni–NO distance so that a direct optical excitation mechanism can be discussed. Table III and Fig. 7 show that there are only very few states with large transition moments and that these transition moments behave differently though all potential curves for the charge transfer states are very similar. The different behavior of the oscillator strengths is difficult to explain in detail, it depends in a rather complex way on the overlap between the NO (2π) orbital and the cluster orbitals out of which the electron is excited.[66]

The differences in the absolute value of the oscillator strengths might be important for the selection of the states which are involved in the desorption process because an optical transition to those states is most likely. Furthermore, even the existence of strongly differing oscillator strengths for similar potential energy curves is an interesting aspect for the relaxation process. It leads us to the assumption that also the diabatic coupling coefficients of nonradiative de-excitation process could in principle be different as a result of different electronic wave functions for the different excited states. This question is also a field for further investigations.[60]

E. Wave packet calculations

In order to simulate the desorption dynamics we have performed some first wave packet calculations. As shown in the previous paragraphs of this section, more than one excited state is involved in the desorption process. This requires the application of a multisurface propagation scheme and the time evolution of the total wave packet has to be treated as a time dependent coherent superposition of wave functions on each surface.

The results of two-dimensional multisurface wave packet calculations including lifetime distributions determined by nonadiabatic coupling coefficients will be pub-

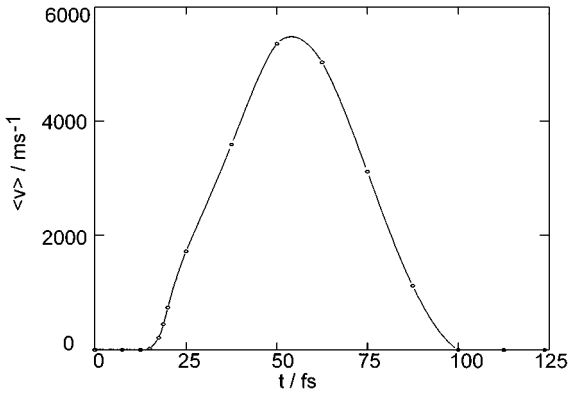

FIG. 8. Velocity of the desorbing NO molecules as a function of lifetime of the excited state. One excited state and fixed lifetimes have been used in these calculation.

lished elsewhere.[72] Here we report preliminary results of one dimensional wave packet calculations on Morse potentials adjusted to our *ab initio* potentials as described in Sec. II C. They should be regarded as a test of our potentials and a comparison with classical trajectory calculations. A fixed lifetime and only one excited state potential was used. In this model quantum interference effects of the multisurface approach are not included, therefore a direct comparison with the classical trajectory calculations of Baumeister and Freund[23] is possible.

The wave functions describing the nuclear motion of the desorbing NO molecules have been analysed as a function of the lifetime of the excited state. The parameters of the calculation are given in Table I. By transforming the wave function into k-space we obtain a momentum distribution that we can compare directly with the velocity flux distributions measured in the experiments.[24,25] Of course, the calculated velocity distributions depend strongly on the lifetime of the wave packet in the excited state. We were able to reproduce the experimentally observed velocities by assuming a mean lifetime between 15 fs to 25 fs (Fig. 8). A shorter lifetime does not lead to desorption at all and a longer lifetime produces particles with much higher velocities than observed experimentally. Very long lifetimes (75 fs–100 fs) could also lead to an agreement with experiment but have been ruled out by the classical trajectory calculations of Baumeister *et al.* because the bimodality as a dominant feature of the velocity-flux distributions could not be reproduced.[58]

The present wave packet calculations are in good agreement with the classical trajectory calculations of Baumeister and Freund[23,58] as far as the lifetimes in the excited state are concerned. Since these authors did not observe essential differences in their calculations with fixed lifetimes and lifetime distributions, we limited the present calculations to a delta function decay.

We have also examined the expectation value of the position operator during the lifetime of the excited state. We found the propagation of the wave packet to take mainly place on the attractive part of the excited state potential which is dominated by the $1/R$ Coulomb attraction. Using this simple model for the desorption process we observed only monomodal wave functions in k-space. This clearly shows that this model is too simple and that either more than one excited state potential curve or a relaxation probability instead of a fixed lifetime have to be used. Furthermore, the inclusion of the rotational coordinate could also affect the shape of the velocity distributions.[58]

IV. CONCLUSIONS

We have calculated potential curves of the ground state and selected excited states for the model system NiO_5^{8-}–NO as functions of the distance between NO and the NiO(100) surface and of the tilt angle between the NO axis and the surface normal. The excited states involved in the laser-induced desorption of NO from NiO(100) were of the form NiO_5^{7-}–NO^-, i.e., surface $\rightarrow$ NO charge transfer states.

The potential curves of all these charge transfer states show the same distance dependence, i.e., a pronounced minimum caused by a strong Coulomb attraction. The equilibrium distance is shifted by 1 a_0 towards the surface, as compared to the ground state. This implies an Antoniewicz like desorption model,[57] i.e., the molecules move towards the surface before they desorb.

All these excited states behave similar to the ground state as far as the tilt angle of the NO molecule against the surface normal is concerned. Thus, the adsorbate molecule cannot be described as a free rotor after laser excitation, as has been assumed in previous model calculations.[58]

We have found a great number of charge transfer states with a high density of states at vertical excitation energies greater than about 8 eV. After a semiempirical shift that accounts for the polarization of the crystal these excitation energies are located in the experimentally accessible energy range of 3.5–6.4 eV. The high density of NO^--like states implies the involvement of more than one excited state in the desorption process.

All surface $\rightarrow$ NO charge transfer states have similar potential curves, but totally different oscillator strengths. This result has led us to consider the possibility of direct optical excitation into the charge transfer states. However, we estimate that for the de-excitation from the charge transfer states back to the ground state nonradiative processes are more likely than radiative processes.

The different velocities of the desorbing NO molecules can be caused by different mean lifetimes, which provides a natural explanation of the bimodal velocity flux distributions observed experimentally.[24,25] However, it should be emphasized that the whole process of the laser-induced desorption might be even more complex. Figure 9 shows a schematic plot of all excited states of the system NiO (100)–NO that might be involved in the process. There are mainly three classes of low-lying states. (1) Local dd excitations within the Ni^{2+} ions whose energies do not depend much on the Ni–N distance, similar to that of the ground state. (2) O($2p$) $\rightarrow$ Ni ($3d$) charge transfer states within the NiO substrate, forming a continuum above the optical band gap at 4 eV, with a distance dependence also similar to that of the ground

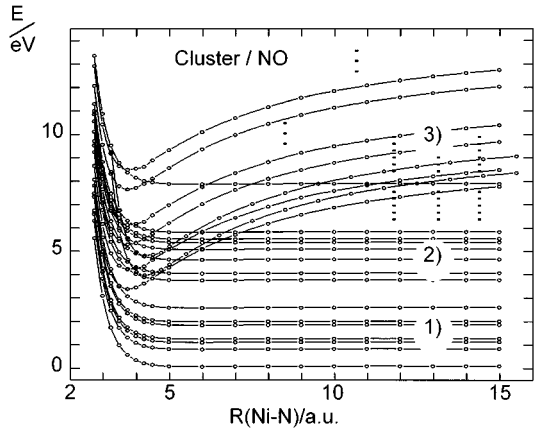

FIG. 9. Schematic plot of the manifolds of potential curves of the different types of excited states of NiO_5^{8-}–NO. (1) Ground state and dd-excitations with a distance behavior similar to that of the ground state. (2) O $2p \rightarrow$Ni $3d$ charge transfer states with a distance behavior which is also similar to that of the ground state. (3) Cluster→NO charge transfer states with a distance behavior dominated by a strong Coulomb attraction.

state. (3) The NiO → NO charge transfer states, as discussed so far in this paper, also a continuum, with a strong Coulomb attraction.

Two different excitation processes seem to be possible which can lead to the NiO^+–NO^- charge transfer. A direct optical transition from the ground state into the manifold of the NiO → NO charge transfer states or a charge transfer excitation within the substrate followed by a nonadiabatic process into the NiO → NO charge transfer states. (''Creation of hot electrons in the substrate which then can be scattered to the NO molecule.'') The same possibilities exist of course also for the deexcitation process. A detailed investigation of this second process would require—apart from the potential curves—the calculation of the diabatic coupling coefficients which will be possible in the future on the basis of recent developments in diabatization procedures.[67–71]

On the basis of our *ab initio* calculations, one can discuss several reasons why laser induced desorption could result in nonmonomodal velocity flux distributions. It seems likely that more than one excited state is involved in the desorption process. If one assumes a direct optical excitation it is possible to decide which of the states are involved via the calculation of oscillator strengths. If, alternatively, the excitation mechanism has to be described as a nonadiabatic process the calculation of diabatic couplings allows in a similar way to identify the states involved. Since the relaxation process is believed to be nonradiative the calculation of nonadiabatic couplings will clarify if the coupling coefficients are also different for different transitions as has been shown for oscillator strengths in this work. Assuming the situation for diabatic couplings and oscillator strengths to be comparable the bimodality can be understood as being due to different coupling of different NO^-/NiO^+-like excited states to the NO/NiO-like manifold of states because different coupling should result in different mean lifetimes of those states which leads naturally to nonmonomodal velocity flux distributions. In addition to this also geometric effects turn out to be important for a complete description of the desorption process.[23]

For the time being we cannot rule out any of the models described above but future calculations of diabtic couplings and more sophisticated wave packet calculations will give us a deeper insight into the fundamental physical principles of the desorption process and may result in a description where all of the models proposed have to be considered to some extent.

ACKNOWLEDGMENTS

The authors thank R. Kosloff and B. Schmidt for allowing the use of their wave packet programs and many helpful discussions. This work was financially supported by the Deutsche Forschungsgemeinschaft through the project ''Modellkat,'' the Ministerium für Wissenschaft und Forschung des Landes Nordrhein-Westfalen, the German–Israeli Foundation (GIF) and the Studienstiftung des deutschen Volkes.

[1] H. Zacharias, Appl. Phys. A **47**, 37 (1988).
[2] F. Träger, in *Photothermal and Photochemical Processes at Surfaces and Thin Films*, Vol. 47 in Topics in Current Physics, edited by P. Hess (Springer, Berlin, 1993).
[3] R. R. Cavanagh, D. S. King, J. C. Stephenson, and T. F. Heinz, J. Phys. Chem. **97**, 786 (1993).
[4] X. L. Zhou and X. Y. White, Surf. Sci. Rep. **13**, 77 (1991).
[5] *Laser Spectroscopy and Photochemistry on Metal Surfaces*, edited by H. L. Dai and W. Ho, Advanced Series in Physical Chemistry (World Scientific, London, 1995), Vol. 5.
[6] K. Al-Shamery, M. Menges, I. Beauport, B. Baumeister, T. Klüner, Th. Mull, H.-J. Freund, C. Fischer, P. Andresen, J. Freitag, and V. Staemmler, in Proceedings of the SPIE'S OE/Laser '94 Conference (in press).
[7] W. Ho, Surf. Sci. **299/300**, 996 (1994).
[8] P. S. Bagus and K. Hermann, Solid State Commun. **20**, 5 (1976).
[9] K. Hermann and P. S. Bagus, Phys. Rev. B **16**, 4195 (1977).
[10] J. N. Allison and W. A. Goddard III, Surf. Sci. **115**, 553 (1982).
[11] G. Pacchioni and P. S. Bagus, J. Chem. Phys. **93**, 1209 (1990).
[12] J. Sauer, P. Ugliengo, E. Garrone, and V. R. Saunders, Chem. Rev. **94**, 2095 (1994).
[13] D. R. Jennison, E. B. Stechel, A. R. Burns, and Y. S. Li, Nucl. Instr. Phys. Res. Sec. B **101**, 22 (1995).
[14] A. D. Becke, Phys. Rev. A **38**, 3098 (1988).
[15] J. P. Perdew, J. A. Chevary, S. H. Vosko, K. A Jackson, M. R. Pederson, D. J. Singh, and C. Fiolhais, Phys. Rev. B **46**, 6671 (1992).
[16] P. A. Schultz and M. P. Sears, Bull. Am. Phys. Soc. **38**, 1439 (1993).
[17] D. R. Jennison, E. B. Stechel, and A. R. Burns, J. Electron Spectrosc. Relat. Phenom, **72**, 9 (1995).
[18] A. R. Burns, E. B. Stechel, D. R. Jennison, and Y. S. Li, J. Chem. Phys. **101**, 6319 (1994).
[19] D. Menzel and R. Gomer, J. Chem. Phys. **41**, 3311 (1964).
[20] P. A. Readhead, Can. J. Phys. **42**, 886 (1964).
[21] M. Pöhlchen and V. Staemmler, J. Chem. Phys. **97**, 2583 (1992).
[22] V. Staemmler, *Adsorption on Ordered Surfaces of Ionic Solids and Thin Films*, edited by H.-J. Freund and E. Umbach (Springer, Berlin, 1993), p. 169.
[23] B. Baumeister and H. -J. Freund, J. Phys. Chem. **98**, 11 962 (1994).
[24] Th. Mull, B. Baumeister, M. Menges, H.-J. Freund, D. Weide, C. Fischer, and P. Andresen, J. Chem. Phys. **96**, 7108 (1992).
[25] M. Menges, B. Baumeister, K. Al-Shamery, H.-J. Freund, C. Fischer, and P. Andresen, J. Chem. Phys. **101**, 3318 (1994).
[26] H. Kuhlenbeck, G. Odörfer, R. Jaeger, G. Illing, M. Menges, Th. Mull, H.-J. Freund, M. Pöhlchen, V. Staemmler, S. Witzel, C. Scharfschwerdt, K. Wennemann, T. Liedte, and M. Neumann, Phys. Rev. B **43**, 1969 (1991).

[27] K. Al-Shamery, I. Beauport, H.-J. Freund, and H. Zacharias, Chem. Phys. Lett. **222**, 107 (1994).
[28] M. Pöhlchen, Ph.D. thesis, Ruhr-University, Bochum, 1992.
[29] L. G. M. Pettersson, Theor. Chim. Acta **87**, 293 (1994).
[30] A. Freitag, V. Staemmler, D. Cappus, C. A. Ventrice Jr., K. Al-Shamery, H. Kuhlenbeck, and H.-J. Freund, Chem. Phys. Lett. **210**, 10 (1993).
[31] D. Cappus, Ph.D. thesis, Ruhr-University, Bochum, 1995.
[32] J. Yoshinubo, X. Guo, and J. T. Yates, Jr., J. Chem. Phys. **92**, 7700 (1991).
[33] H.-J. Freund, *Clean and Modified Oxide Surfaces: Structure and Dynamics of Adsorbed Molecules*, in Metal–Ligand Interactions: Structure and Reactivity, Nato Advanced Study Institute, edited by N. Russo and D. R. Salahub (Kluwer, Dordrecht, 1996), Vol. C474, p. 233.
[34] R. W. G. Wyckoff, *Crystal Structures*, 2nd ed. (Interscience, New York, 1965), Vol. I, p. 89.
[35] M. A. van Hove, S.-W. Wang, D. F. Ogletree, and G. A. Somorjai, Adv. Quantum Chem. **20**, 1 (1989).
[36] H. M. Evjen, Phys. Rev. **39**, 675 (1932).
[37] J. Freitag and V. Staemmler, J. Electron Spectrosc. Relat. Phenom. **69**, 99 (1994).
[38] T. Klüner, Diplomarbeit, Ruhr-University, Bochum, 1994.
[39] P. Boussard, P. E. M. Siegbahn, and U. Wahlgren, *Adsorption on Ordered Surfaces of Ionic Solids and Thin Films*, edited by H.-J. Freund and E. Umbach (Springer, Berlin, 1993), p. 192.
[40] V. Staemmler, Theor. Chim. Acta **45**, 89 (1977).
[41] U. Meier and V. Staemmler, Theor. Chim. Acta **76**, 95 (1989).
[42] J. Wasilewski, Int. J. Quantum Chem. **36**, 503 (1989).
[43] V. Staemmler and R. Jaquet, Theor. Chim. Acta **59**, 487 (1981).
[44] R. J. Gdanitz and R. Ahlrichs, Chem. Phys. Lett. **143**, 413 (1988).
[45] R. Fink and V. Staemmler, Theor. Chim. Acta **87**, 129 (1993).
[46] B. Roos, A. Veillard, and G. Vinot, Theor. Chim. Acta **20**, 1 (1971).
[47] S. Huzinaga (reprint, University of Alberta, Canada, 1971).
[48] S. F. Boys and F. Bernardi, Mol. Phys. **19**, 553 (1970).
[49] R. Kosloff, J. Phys. Chem. **92**, 2087 (1988).
[50] H. Tal-Ezer and R. Kosloff, J. Chem. Phys. **81**, 3967 (1984).
[51] D. Kosloff and R. Kosloff, J. Comp. Phys. **63**, 363 (1986).
[52] R. Bisseling and R. Kosloff, J. Comp. Phys. **59**, 136 (1985).
[53] R. Kosloff and H. Tal-Ezer, Chem. Phys. Lett. **127**, 223 (1986).
[54] R. Kosloff and D. Kosloff, J. Chem. Phys. **79**, 1823 (1983).
[55] G. J. M. Janssen and W. C. Nieuwpoort, Phys. Rev. B **38**, 3449 (1988).
[56] A. Fujmori and F. Minami, Phys. Rev. B **30**, 957 (1984).
[57] P. R. Antoniewicz, Phys. Rev. B **43**, 3811 (1980).
[58] B. Baumeister, Ph.D. thesis, Ruhr-University, Bochum, 1994.
[59] E. Hasselbrink, Chem. Phys. Lett. **170**, 329 (1990).
[60] T. Klüner, Ph.D. thesis, Ruhr-University Bochum (in preparation).
[61] J. W. Gadzuk, L. J. Richter, S. A. Buntin, D. S. King, and R. R. Cavanagh, Surf. Sci. **235**, 317 (1990).
[62] G. W. Bethke, J. Chem. Phys. **31**, 662 (1959).
[63] A. Pery-Thorne and F. P. Banfield, J. Phys. Ser. B **3**, 1011 (1970).
[64] V. Hasson and R. W. Nicholls, J. Phys. Ser. B **4**, 1769 (1971).
[65] A. J. D. Farmer, V. Hasson, and R. W. Nicholls, J. Quantum Spectrosc. Radiat. Transfer **12**, 635 (1972).
[66] J. Freitag, Ph.D. thesis, Ruhr-University Bochum (in preparation).
[67] B. H. Lengsfield III and D. R. Yarkony, *Advances in Chemical Physics*, edited by M. Baer and C.-Y. Ng (Wiley, New York, 1992), Vol. LXXXII, Part 2, p. 1.
[68] T. Pacher, L. S. Cederbaum, and H. Köppel, *Advances in Chemical Physics*, edited by I. Prigogine and S. A. Rice (Wiley, New York, 1993), Vol. LXXXIV, p. 293.
[69] T. Pacher, L. S. Cederbaum, and H. Köppel, J. Chem. Phys. **89**, 7367 (1988).
[70] T. Pacher, L. S. Cederbaum, and H. Köppel, J. Chem. Phys. **95**, 6668 (1991).
[71] W. Domcke, C. Woywod, and M. Stengle, Chem. Phys. Lett. **226**, 257 (1994).
[72] T. Klüner, R. Kosloff, V. Staemmler, and H.-J. Freund (unpublished).